Graphical abstract

Circular dichroism of anthocyanidin 3-glucoside self-aggregates

Raquel Gavara, Vesselin Petrov, Alexandre Quintas, Fernando Pina *

The circular dichroism spectra of the six most common anthocyanidin 3-glucoside show the formation of left handed aggregates compatible with dimers. The absorption bands of the monomer split by increasing concentration according to the formation of H and J aggregates. The angle and distance between the transition moments of the two monomers in the dimer was calculated from the splitting of the 0–0 absorption band. While the angle is similar for the series the distance changes dramatically. The intensity of the CD signal is proportional to the inverse of the square of the distance.

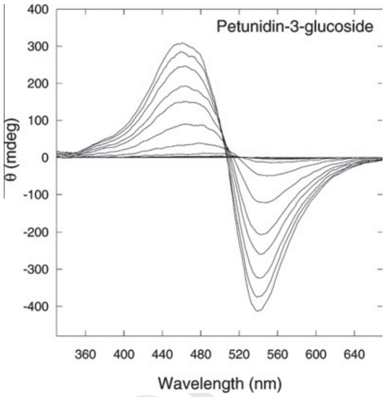

Highlights

Q10 ▶ The circular dichroism spectra of six common anthocyanins 3-glucosides was obtained. ▶ Like 3,5-diglucoside analogous they exhibit left-handed CD signals. ▶ J and H aggregates are formed by concentration increasing. ▶ The distance of the transition moments correlate with the intensity of the CD signal.

Circular dichroism of anthocyanidin 3-glucoside self-aggregates

Raquel Gavara[a], Vesselin Petrov[a], Alexandre Quintas[b], Fernando Pina[a,]*

[a] REQUIMTE, Departamento de Química, Faculdade de Ciências e Tecnologia, Universidade Nova de Lisboa, 2829516 Monte de Caparica, Portugal
[b] Instituto Superior de Ciencias da Saude Egas Moniz, Centro de Investigação Interdisciplinar Egas Moniz, P-2829511 Monte de Caparica, Caparica, Portugal

A R T I C L E   I N F O

Keywords:
Circular dichroism
Anthocyanins
J and H aggregates

A B S T R A C T

Self-association constants for the flavylium cations of the six most common anthocyanidin 3-glucosides were determined by circular dichroism (CD) and UV–Vis spectroscopy. Along with previous ^{1}H NMR results, all measurements were consistent with a monomer–dimer model. The CD spectra of the anthocyanidin 3-glucosides were similar to the analogues 3,5-diglucosides. All dimers of the anthocyanidin 3-glucosides exhibited left-handed CD signals, with petunidin-3-glucoside and myrtillin having the most intense signals. In addition, the magnitude of the molar ellipticity, $[\theta]$, was generally higher for the 3-glucosides than for the 3,5-diglucosides. For all six anthocyanins studied, the CD absorption spectra of their dimers showed evidence of the splitting of the monomer absorption into lower (J) and higher (H) energy bands. The angle and the distance between the dipolar moments of the two monomers comprising the dimer were obtained from the lower energy absorption band.

While the angle was more or less similar in all six dimers, the separation distance between the monomer dipole moments differed dramatically. The intensity of the CD signal displayed a linear dependence with the inverse square of the dipole moment distances.

1. Introduction

Anthocyanins are the pigments responsible for the beautiful red to blue colours of flowers and fruits. However, when their pH dependent equilibrium is studied in water at low concentrations, the red flavylium cation is only stable at very acidic pH values, while the blue quinoidal base is a minor species (<5%) at moderately acidic ones. Due to the fact that the pH of the vacuoles, where anthocyanins are located, changes roughly from 3 to 6 (Steward et al., 1975) some kind of interactions that permit to achieve colour in these conditions must take place. One solution found by Nature regarding the achievement of blue colour, is the formation of supramolecular structures involving metals and flavonoids, which are able to stabilize the blue quinoidal base (Yoshida et al., 1995, 2009).

In the case of red colour it was reported for raspberry the presence of high concentrations of cyanidin 3-glucoside (kuromanin, ca. 2.4 mg/g of fresh fruit) and other derivatives bearing different sugars in position 3 (Melo et al., 2000). Nature uses high concentrations of the anthocyanin to compensate for the fact that is not using the total colouring power of the flavylium cation (for pH 3.1 found in raspberry extract, the mole fraction of flavylium cation of the cyanidin 3-glucoside is only ca. 0.33). The use of high concentration of anthocyanins (Wu et al., 2006), in particular anthocyanidin 3-glucosides, raises the question of self-aggregation and its influence on the colour definition.

In a series of papers Hoshino et al. (1982) demonstrated that anthocyanidin 3,5-diglucosides self-aggregate by stacking in a right-handed or left-handed screw axis. While quinoidal bases of cyanin and pelargonin lead to right-handed adducts, peonin, delphin and malvin form left-handed ones. On the other hand, all the respective flavylium cations lead to aggregates exhibiting left-handed CD signals, due to a super-asymmetry imposed by the oligomeric species (Rodger and Nordén, 1997).

In a recent paper we have carried out an extended studied of the self-aggregation in the six most abundant anthocyanidin 3-glucosides (Leydet et al., in press), by means of ^{1}H NMR and UV–Vis absorption. It was verified that the rate and equilibrium constants of the network of chemical reactions involving the dyes is dramatically dependent on the anthocyanin concentration. In this work we report the circular dichroism spectra of these compounds, Scheme 1, and correlate the magnitude of the CD signal with the angle and distance between the dipolar moments of the monomers in the dimer.

2. Experimental

Myrtillin chloride, oenin chloride, kuromanin chloride and callistephin chloride were purchased from Extrasynthèse; peonidin-3-glucoside chloride and petunidin-3-glucoside chloride were purchased from PhytoLab. All the reagents (⩾95%) were used

---

* Corresponding author.
E-mail address: fp@fct.unl.pt (F. Pina).

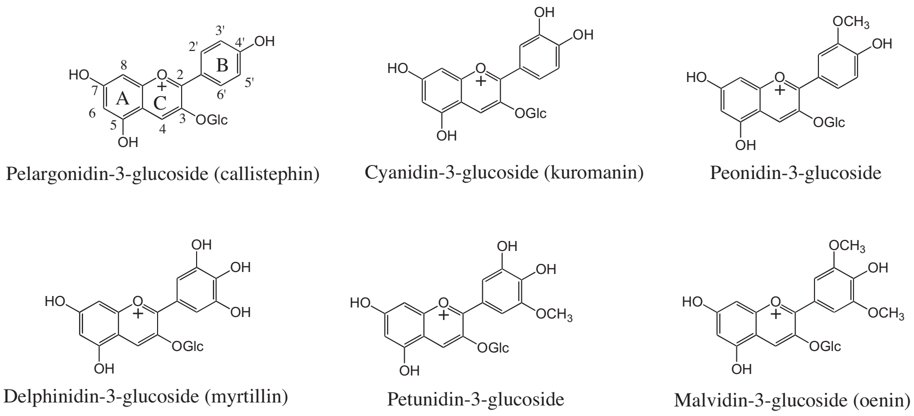

Scheme 1. The six anthocyanidin 3-glucosides.

without any further purification. The solutions were prepared in Millipore water, and HCl 0.1 M was employed to acidify the samples at pH 1.

UV–Vis absorption spectra were recorded on Varian Cary 100 Bio, Varian Cary 5000i and Jasco V-530 spectrophotometers.

2.1. Circular dichroism analysis

Myrtillin chloride, oenin chloride, kuromanin chloride, callistephin chloride, peonidin-3-glucoside chloride and petunidin-3-glucoside solutions at pH 1 were prepared 12 h before the experiments and kept at 4 °C.

Circular dichroism were performed using near-UV and visible (350–700 nm) CD in a Jasco J810 spectropolarimeter equipped with a temperature control unit Julabo F25 using a range of concentration of the different 3-glucoside anthocyanins from 10^{-3} to 10^{-6} M. Near-UV and visible CD spectra were recorded with 0.01, 0.05, 0.1 and 1 cm (linear) path length quartz cuvette at 20 °C, according to the measured high tension (HT) voltage measured in each sample. For each spectrum, three scans were averaged and anthocyanidin 3-glucosides concentration was checked by absorbance at the maximum in the visible region using the molar absorption coefficients of each flavylium cation under study (myrtillin chloride, oenin chloride, kuromanin chloride, callistephin chloride, peonidin-3-glucoside chloride and petunidin-3-glucoside chloride) on a UV–Vis spectrophotometer Jasco V-530.

Molar ellipticity for each compound has been calculated using the formulae:

$$[\theta] = \theta/(C.l.10)\,\text{deg cm}^2\,\text{dmol}^{-1}$$

where θ is the ellipticity (mdeg), C the concentration (mol l^{-1}) and l the path length (cm).

CD spectra of the appropriate blanks (HCl 0.1 M) were recorded and subtracted from the anthocyanidin 3-glucosides spectra.

3. Results and discussion

3.1. Circular dichroism

The circular dichroism spectra representing the ellipticity of petunidin-3-glucoside at pH 1.0 is shown in Fig. 1A. The molar ellipticity at the maximum of the first and second cotton bands is represented in Fig. 1B. The same is shown for oenin (malvidin 3-glucoside) in Fig. 2A and B. Identical figures for the four remaining anthocyanins of Scheme 1, are reported in Supplementary material, Fig. S1–S4. At lower concentrations the molar ellipticity

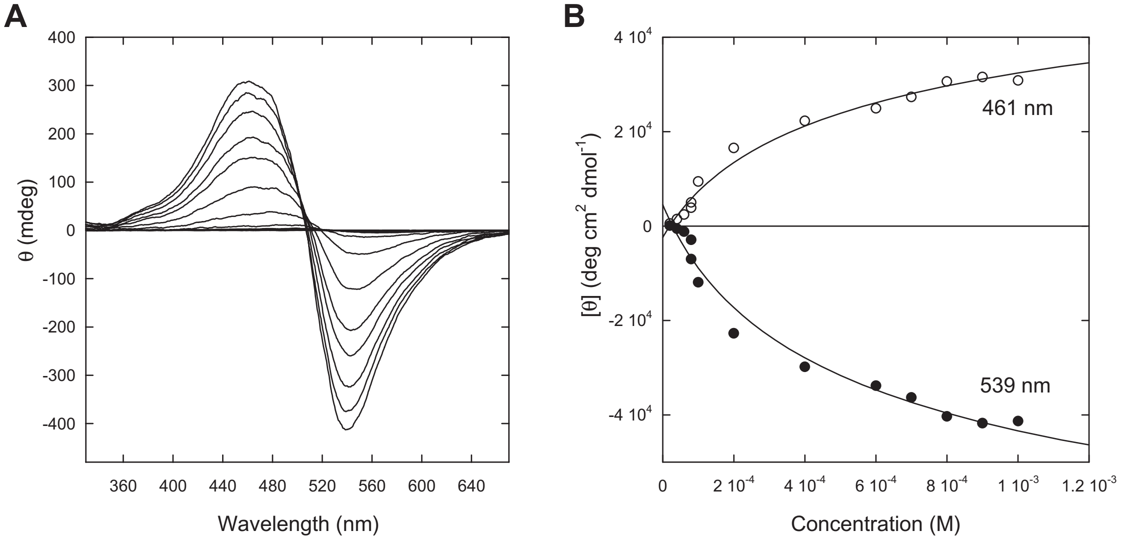

Fig. 1. (A) Ellipticity of petunidin-3-glucoside as a function of concentration (up to 10^{-3} M); (B) molar ellipticity at the first (539 nm) and second (461 nm) cotton bands. $K_D = 900\ M^{-1}$.

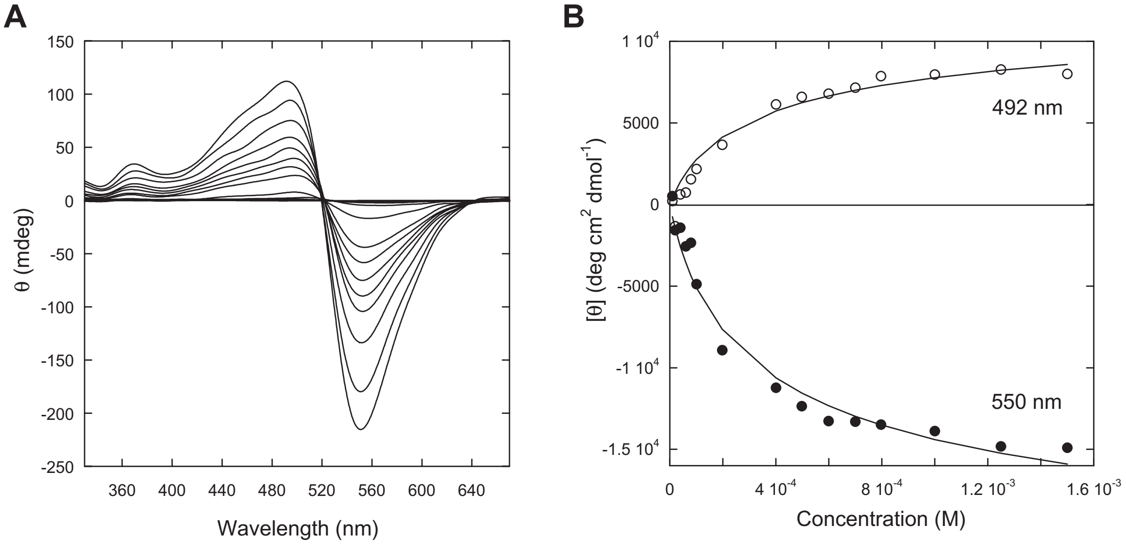

Fig. 2. (A) Ellipticity of oenin as a function of concentration (up to 1.5×10^{-3} M); (B) Molar ellipticity at the first (550 nm) and second (492 nm) cotton bands. $K_D = 976\ \mathrm{M}^{-1}$.

Table 1
Ellipticity data for the six anthocyanidin 3-glucosides.[a]

Anthocyanin	[θ]1st Cotton (deg cm^2 dmol^{-1})	[θ] 2nd Cotton (deg cm^2 dmol^{-1})	$\varepsilon_{\mathrm{dimer}}$/M^{-1} cm^{-1} ($\lambda_{\max}$)	Corrected CD intensity[b]
Myrtillin	−76,610 (539 nm)	57,870 (452 nm)	28,600 (483 nm)	2.8
Oenin	−29,550 (550 nm)	16,830 (492 nm)	40,300 (514 nm)	3.3
Petunidin	−94,740 (539 nm)	69,820 (461 nm)	41,700 (497 nm)	1.1
Kuromanin	−55,130 (539 nm)	25,000 (452 nm)	22,700 (503 nm)	1.7
Peonidin	−26,300 (541 nm)	13,310 (466 nm)	41,100 (503 nm)	4.0
Callistephin	−19,080 (529 nm)	13,610 (414 nm)	56,220 (496 nm)	0.58

[a] Obtained form the fitting of Fig. 1B and B and the equivalent figures in supplementary material.
[b] Calculated as the sum of the maximum of the absolute value of the 1st and 2nd Cotton bands divided by the mole absorption coefficient of the dimer, see below.

in the visible region is practically zero, indicating that the monomer does not exhibit signal. Signal rises when concentration increases due to the appearance of supramolecular chirality upon aggregation.

The fittings of the molar ellipticity of all the six anthocyanins were achieved using a monomer–dimer model (see below) and the dimerization constants previously calculated by ^{1}H NMR, (Leydet et al., in press).

As shown in Figs. 1 and 2 (as well as Fig. S1–S4 in Supplementary material) the flavylium cation adducts of the six anthocyanidin 3-glucosides of Scheme 1, self-associate in a left-handed manner, as reported for the 3,5-diglucoside analogues (Hoshino, 1982). The CD strongest signal occurs for petunidin-3-glucoside and delphinidin-3-glucoside (myrtillin) similarly to what was previously observed for the 3,5-diglucoside analogous. However, comparison with the molar ellipticity, [θ], of 3,5-diglucosides seems to indicate that 3-glucosides exhibit in general a higher [θ]. This suggests that the crucial sugar to form the screw is the one in position 3. The presence of a second sugar in position 5 of the flavylium cation seems to have a small effect on the intensity of the CD signal, and thus the screw shape and the respective ellipticity is essentially modulated by the sugar in position 3.

It is worth of note the fact that the intensity of the CD signal is not proportional to the value of the aggregation constant: for example oenin possesses a high association constant but presents a weak CD signal. Two main factors contribute to the appearance of the CD signal: (i) the distance between the dipolar moments of the two monomers, more properly the inverse of the square of the distance; (ii) the angle formed between the dipolar moments of the molecules during aggregation stacking. Additionally, the CD signal is also proportional to the molar absorption coefficient of the chromophore, in this case the dimer adduct (Berova and Di Bari, 2007).

In order to normalize the effect of the chromophore absorption on the CD signal, a "corrected" CD intensity was calculated by considering the sum of the molar ellipticity around the maximum of the 1st and 2nd cotton bands (amplitude) divided by the molar absorption coefficient of the dimer $\varepsilon_{\mathrm{dimer}}$/M^{-1} cm^{-1} (see below) taken at the maximum (Table 1).

3.2. ^{1}H NMR

In a recent paper (Leydet et al., in press) we reported that the ^{1}H NMR peaks of the protons H_4, H_6 and H_8 of the flavylium cation of anthocyanidin 3-glucosides are dramatically shifted to high field by increasing concentration. This is a result of the shielding of these protons upon aggregation, a phenomenon previously observed by other authors (Hoshino, 1992; Hoshino et al., 1982; Houbiers et al., 1998), see Supplementary material for the ^{1}H NMR data. The difference between the chemical shift of the dimer and monomer, Table 2, suggests that protons H_4 and H_6 are more affected than proton H_8 by the interaction in the aggregate, and this should be an important clue for the determination of the dimer structure.

The ^{1}H NMR data of the six anthocyanidin 3-glucosides (Leydet et al., in press) was treated with a monomer–dimer and isodesmic models (Dimicoli and Hélène, 1973) the last one considering the existence of higher order aggregates with the same association

Table 2
Variation of the chemical shifts from the dimer to the monomer obtained by ^{1}H NMR (Leydet et al., 2011).

Anthocyanin	H_4	H_6	H_8
Myrtillin	1.06	0.96	0.54
Oenin	0.73	0.78	0.49
Petunidin-3-glucoside	1.27	1.2	0.69
Kuromanin	0.75	0.7	0.4
Peonidin-3-glucoside	0.89	0.75	0.51
Callistephin	0.47	0.44	0.31

constant. In both cases good fittings have been obtained and the ^{1}H NMR data was not able to discriminate between the two models.

3.3. Monomer–dimer model

Similarly to the data of the ^{1}H NMR, the circular dichroism spectra presented in this work was also treated with a monomer–dimer model, as follows:

The monomer (M)–dimer (D) equilibrium is described by Eq. (1):

$$M + M \leftrightarrow D \tag{1}$$

and the dimeric constant (K_D) is defined by Eq. (2):

$$K_D = \frac{[D]_{eq.}}{([M]_{eq.})^2} = \frac{\chi^D_{eq.}}{2C^0_{eq.} \cdot (\chi^M_{eq.})^2} \tag{2}$$

Considering the mass balance of the system given by Eq. (3):

$$[M]_{eq.} + 2[D]_{eq.} = C^0_{eq.} \tag{3}$$

$$\chi^M_{eq.} + \chi^D_{eq.} = 1$$

where the molar fractions (χ) are defined according the Eqs. (4) and (5):

$$\chi^M_{eq.} = \frac{[M]_{eq.}}{C^0_{eq.}} = \frac{-1 + \sqrt{1 + 8C^0_{eq.}K_d}}{4K_d C^0_{eq.}} \tag{4}$$

$$\chi^D_{eq.} = \frac{2[D]_{eq.}}{C^0_{eq.}} \tag{5}$$

Finally, the molar ellipticity of the system is defined as:

$$[\theta] = [\theta]_M \chi_M + [\theta]_D \chi_D \tag{6}$$

where $[\theta]$ is the 1st or 2nd cotton bands signal $[\theta]_M$ the CD signal of the monomer ($\approx$0) and $[\theta]_D$ the molar ellipticity of the dimer.

Fitting was achieved for the same set of constants calculated on the basis of the ^{1}H NMR chemical shifts (Leydet et al., in press), see Table 3. However, good fittings are also obtained using the isodesmic model which implies the formation of *n*-Mers with identical successive association constants. Consequently, it cannot be excluded the formation of higher order aggregates, but the accuracy of the data does not allow discrimination between monomer–dimer and alternative models. It is worth to comment that this conclusion cannot be extended, in principle, to the self-aggregation of the quinoidal base, where indirect evidence to the formation of higher order aggregates was obtained (Hoshino et al., 1981a,b). Regarding to the flavylium cation it is possible that its positive charge hinders the association of the dimer with additional monomers, because of the growing electrostatic repulsion.

The following discussion will be carried out using the monomer–dimer model.

Table 3
Angle and distance between the dipole moments of monomers in dimers (calculated from the 0–0 electronic absorption band). [f]

Anthocyanin	K_D (M^{-1})[a]	0–0 Band				
		λ_M (nm)[b]	λ_J (nm)[c]	λ_H (nm)[d]	Angle[e] (°)	Distance[e] (Å)
Myrtillin	1240	529	572	497	−100	2.9
Oenin	976	532	562	519	−128	5.2
Petunidin-3-glucoside	900	531	569	498	−97	2.5[e]
Kuromanin	700	525	558	495	−103	3.2
Peonidin-3-glucoside	661	526	557	495	−114	3.2
Callistephin	404	508	529	475	−110	4.5

[a] Same constants of the ^{1}H NMR studies (Leydet et al., in press).
[b] Absorption maximum of the monomer.
[c] Absorption maximum of the J-band.
[d] Absorption maximum of the H-band.
[e] Estimated error in the angle ± 10°; distance ± 0.2 Å: on the basis of the equations involved, the distance error increases when the angle approaches 90° and this value could be underestimated.
[f] The sign of the anthocyanidin 3-glucoside self-aggregates overlay angle is negative because the front molecule covers the rear molecule in an anti-clockwise turn around an axis coinciding with the distance of the molecules (Klyne and Prelog, 1960).

3.4. UV–Vis absorption

The effect of the aggregation in the UV–Vis absorption spectra is clearly observed when the molar absorption coefficients ε (M^{-1} -cm^{-1}), are represented as a function of the anthocyanin concentration, see Fig. 3A for petunidin-3-*O*-glucoside and Fig. 3B for oenin.

Inspection of Fig. 3 shows the splitting of the monomer absorption in two new red and blue shifted absorptions upon aggregation, see below. The individual spectra of the monomer and dimer in the visible region were obtained as reported previously (Cruz et al., 2010). Thus, a set of absorption spectra at several concentrations (the same range of concentrations employed in the CD measurements) was treated by FiNAl algorithm (Antonov and Petrov, 2002; Antonov et al., 1999). Taking into account the dimerization constant, this algorithm recovers the individual spectrum of the monomer and dimer and gives their contribution (mole fraction) for each concentration. The monomer and dimer absorption bands were additionally deconvoluted using Gaussian functions, see Fig. 4 for oenin as an illustrative example.

The absorption spectrum of the monomer, Fig. 4A, shows the existence of two transitions, the one of lower energy exhibiting two vibrational bands (for example, in the case of oenin, the distance between the vibration maxima (532 and 505 nm) corresponds to 1005 cm^{-1}). Decomposition of the dimer of each anthocyanin was achieved using six bands, Fig. 4B. Each of the monomer absorption bands splits into new bands, corresponding to H and J aggregates (Spano, 2010). [1] The situation is illustrated in Scheme 2.

In the present paper calculations of the distance and angle were performed on the 0–0 absorption band (532 nm for oenin in Fig. 4A), following the Kasha theory (Kasha et al., 1965). It is important to stress that the following calculations do not predict the relative position of the two monomers in the dimer, but the distance and angle between the respective transition dipole moments. Moreover, the position of the transition moment of the monomers

---

[1] H-aggregates are obtained when dye molecules aggregate following a sandwich-type arrangement and J aggregates when the monomer associates in a head-to-tail arrangement. H aggregates lead to a bathochromic shift of the absorption band of the dye, whereas J aggregates originate a hypsochromic shift.

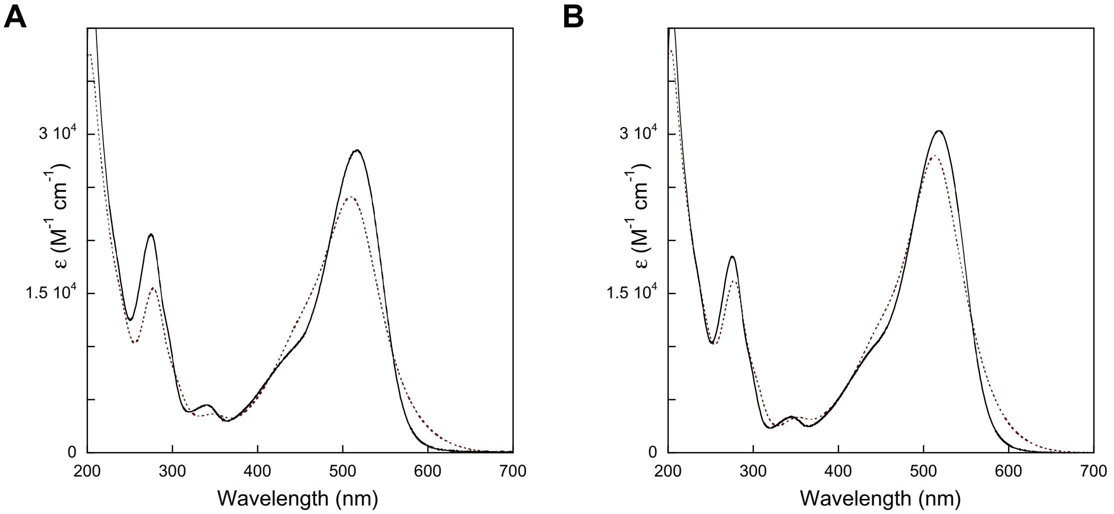

Fig. 3. Representation of the molar absorption coefficient, ε (M^{-1} cm^{-1}), as a function of the anthocyanin concentration: (A) petunidin-3-glucoside 2.0×10^{-5} M (full line) and 7.0×10^{-4} M (pointed line); (B) the same for oenin 2.0×10^{-5} M (full line) and 9.0×10^{-4} M (pointed line).

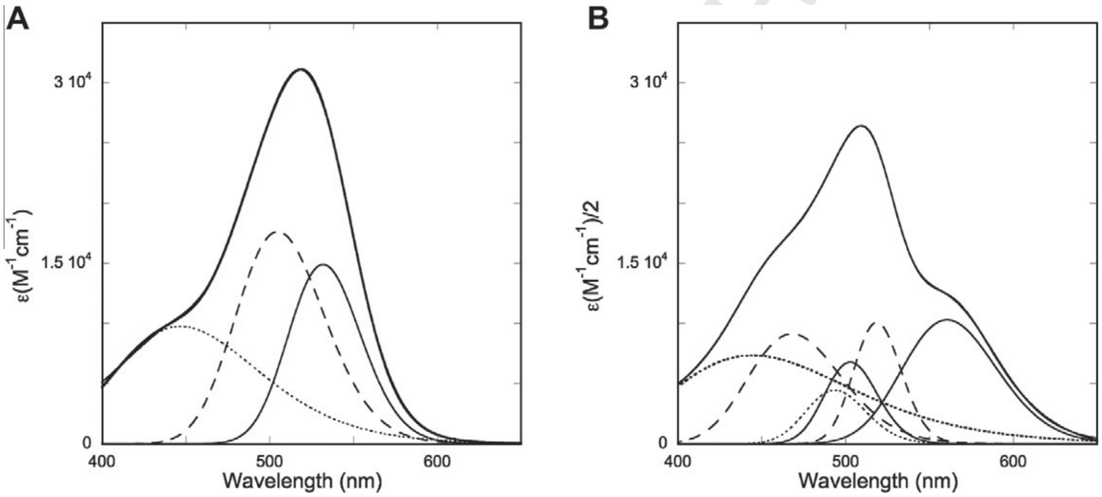

Fig. 4. (A) Spectral decomposition of the monomer of oenin. Vibrational bands of the first absorption 0–0 (full line) and 0–1 (traced line); second singlet (pointed line): (B) spectral decomposition of the three bands upon aggregation (dimer). Each band of the monomer splits in two bands corresponding to J and H aggregates.

in each anthocyanin could be slightly different, due to the different substitution pattern.

3.5. Calculations

The two H and J absorption bands of the dimer were obtained by spectral decomposition and the angle and distance between the transition moments can be interpreted through the exciton model using Eqs. (7) and (8), where the angle (α) between the transitions moments is defined by:

$$\alpha = 2.\arctan\sqrt{\frac{v_H \cdot f_J}{v_J \cdot f_H}} \tag{7}$$

and the distance (R in Å) between the monomers in the dimer is defined by the expression:

$$R = \sqrt[3]{\frac{2.14 \times 10^{10} \cdot \cos\alpha \cdot f_M}{\Delta v \cdot v_M}} \tag{8}$$

v_x is position of the band X in cm^{-1} f_X is oscillator straight defined as $f_X = 1.3 \times 10^{-8}\Theta(n)\int_{-\infty}^{\infty}\varepsilon(v)dv$, $\Theta(n) = \frac{9.n}{(n^2+2)^2}$ is factor of the environment, n is refraction index, $\Delta\tilde{v}$ is the difference of the positions of the split bands (J and H) in cm^{-1}

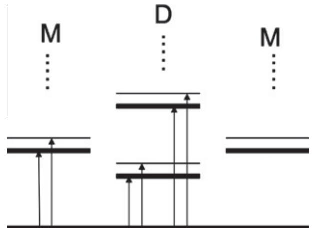

Scheme 2. Splitting of the lower energy band of the monomer upon aggregation in a dimer, including the vibronic bands.

The control of the spectral decomposition can be made by the coincidence, within experimental error, of the energy of the absorption maximum of the monomer and the semi sum of the identical energies of the H and J bands.

In Table 3, the results for the six anthocyanidin 3-glucosides are shown.

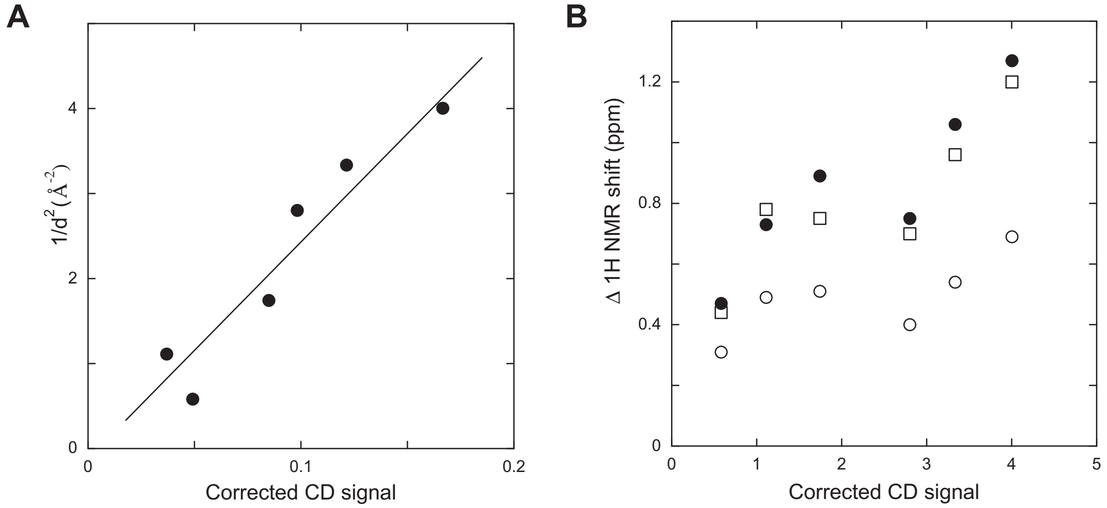

Fig. 5. (A) Representation of the inverse of the square of the distance as a function of the corrected CD signal leads to a relatively good linear relation; (B) representation of the difference between the chemical shifts of the monomer and dimer for protons H4 (●), H6 (□) and H8 (○) as a function of the corrected CD signal.

Inspection of Table 3 suggests that in the case of the 0–0 band the angle between the transition moments of the monomers in the dimer are similar and thus the distance should be the crucial parameter to account for the CD signal. According to the theory, the intensity of the CD signal is proportional to the inverse of the square of the distance (Berova and Di Bari, 2007) and such a relation was observed, as shown in Fig. 5A.

Calculations based on the exciton model have been questioned, in particular when distances lower than Van Der Waals (3.5 Å) are obtained (Arik and Onganer, 2003).[2] However, the existence of hydrogen bonds could lead to shorter values. In addition, anthocyanins are not planar molecules and by consequence their dipole moments are predicted to be out of the plane formed by ring A and C. It is possible to conceive geometries where the two dipoles are closer than the atoms of the whole molecule, if the dimers interact through the same face.

In Fig. 5B the plot of the difference between the chemical shift of the monomer and dimer for protons H_4, H_6 and H_8 (Table 2) as a function of the corrected CD signal suggests, in spite of the great dispersion, that the increasing of the CD signal and the magnitude of the chemical shifts follow the same trend.

4. Conclusion

The self-aggregation of the flavylium cation of the six most common anthocyanidin 3-glucosides is responsible for the chemical shift variations observed in the ^{1}H NMR spectra, appearance of a CD signal characteristic of a left-handed aggregation and split of the UV–Vis absorption band in two other bands (red and blue shifted). In terms of the consequences on the colour expression in plants, the splitting of the absorption bands upon aggregation leads to a slight modification of the colour tonality. Moreover, aggregation stabilizes the colour arising from the flavylium cation because the nucleophilic attack of water occurs at higher pH values. The three techniques (NMR, CD and UV–Vis) lead to self-consistent results and are compatible with a monomer–dimer aggregation type for the flavylium cation. One possible explanation for the apparent lack of high order aggregates is the positive charge of the flavylium cation, which prevents the addition of more monomers to the dimer, due to the increasing electrostatic repulsion.

5. Uncited references

Goto et al. (1976), Hoshino (1991), Hoshino and Goto (1990) and Hoshino et al. (1980). Q6

Appendix A. Supplementary data

Supplementary data associated with this article can be found, in the online version, at http://dx.doi.org/10.1016/j.phytochem.2012.12.011.

References

Antonov, L., Petrov, V., 2002. Quantitative analysis of undefined mixtures – “fishing net” algorithm. Anal. Bioanal. Chem. 374, 1312–1317.

Antonov, L., Gergov, G., Petrov, V., Kubista, M., Nygren, J., 1999. UV–Vis spectroscopic and chemometric study on the aggregation of ionic dyes in water. Talanta 49, 99–106.

Arik, M., Onganer, Y., 2003. Molecular excitons of pyronin B and pyronin Y in colloidal silica suspension. Chem. Phys. Lett. 375, 126–133.

Berova, N., Di Bari, L., 2007. Application of electronic circular dichroism in configurational and conformational analysis of organic compounds. Chem. Soc. Rev. 36, 914–931.

Cruz, L., Petrov, V., Teixeira, N., Mateus, N., Pina, F., Freitas, V., 2010. Establishment of the chemical equilibria of different types of pyranoanthocyanins in aqueous solutions. Evidence for the formation of aggregation in pyranomalvidin-3-*O*-coumaroylglucoside-(+)-catechin. J. Phys. Chem. B 114, 13232–13240.

Dimicoli, J.-L., Hélène, C., 1973. Complex-formation between purine and indole-derivatives in aqueous-solutions-proton magnetic-resonance studies. J. Am. Chem. Soc. 95, 1036–1044.

Goto, T., Hoshino, T., Ohba, M., 1976. Stabilization effect of natural salts on anthocyanins: flavylium salts, anhydrobases and genuine anthocyanins. Agric. Biol. Chem. 40, 1593–1596.

Hoshino, T., 1991. Anthocyanin self-aggregates. 6. An approximation estimate of self-association constants and the self stacking of malvin quinonoidal bases studied by H-1-NMR. Phytochemistry 30, 2049–2055.

Hoshino, T., Goto, T., 1990. Effects of pH and concentration on the self-association of malvidin quinonoidal base – electronic and circular dichroic studies. Tetrahedron Lett. 31, 1593–1596.

Hoshino, T., Matsumoto, U., Goto, T., 1980. Evidence for self-association of anthocyanins. 1. Circular dichroism of cyanin anhydrobase. Tetrahedron Lett. 21, 1751–1754.

Hoshino, T., Matsumoto, U., Goto, T., 1981a. Evidence for self-association of anthocyanins. 2. Self-association of some anthocyanins in neutral aqueous-solution. Phytochemistry 120, 1971–1976.

Hoshino, T., Matsumoto, U., Harada, N., Goto, T., 1981b. Chiral excitation couple stacking of anthocyanins. Interpretation of the origin of anomalous CD induced by anthocyanin association. Tetrahedron Lett. 22, 3621–3624.

Hoshino, T., Matsumoto, U., Goto, T., 1982. Evidence for self-association of anthocyanins. 4. PMR spectroscopic evidence for the vertical stacking of anthocyanin molecules. Tetrahedron Lett. 23, 433–436.

---

[2] We thank the referee who raised this question.

Houbiers, C., Lima, J.C., Maçanita, A.L., Santos, H., 1998. Color stabilization of malvidin 3-glucoside: self-aggregation of the flavylium cation and copigmentation with the Z-chalcone form. J. Phys. Chem. B 102, 3578–3585.

Kasha, M., Rawls, H.R., Ashraf El-Bayoumi, M., 1965. The exciton model in molecular spectroscopy. Pure Appl. Chem. 11, 371–392.

Klyne, W., Prelog, V., 1960. Description of steric relationships across single bonds. Experientia 16, 521–523.

Leydet, Y., Gavara, R., Petrov, V., Diniz, A. M., Parola, A. J., Lima, J. C., Pina, F., in press. The effect of self-aggregation on the determination of the kinetic and thermodynamic constants of the network of chemical reactions in 3-glucoside anthocyanins. Phytochemistry. **Q7**

Melo, M.J., Moncada, M., Pina, F., 2000. On the red colour of Raspberry (*Rubus idaeus*). Tetrahedron Lett. 41, 1987–1991.

Rodger, A., Nordén, B., 1997. Circular Dichroism and Linear Dichroism. Oxford University Press, Oxford.

Spano, F.C., 2010. The spectral signatures of Frenkel Polarons in H- and J-aggregates. Acc. Chem. Res. 43, 429–439 (And references therein).

Steward, R.N., Norris, K.H., Asen, S., 1975. Microspectrophotometric measurements of pH and pH effect on color of petal epidermal-cells. Phythochemistry 14, 937–942.

Wu, X., Beecher, G.R., Holden, J.M., Haytowitz, D.B., Gebhart, S.E., Prior, R.L., 2006. Concentrations of anthocyanins in common foods in the United States and estimation of normal consumption. Agric. Food Chem. 54, 4069–4075.

Yoshida, K., Kondo, T., Okazaki, Y., Katou, K., 1995. Cause of blue petal color. Nature 373, 291.

Yoshida, K., Mori, M., Kondo, T., 2009. Blue flower color development by anthocyanins: from chemical structure to cell physiology. Nat. Prod. Rep. 26, 884–915.